Thermal conductivity of MgB_2 in the superconducting state

M.Putti, V.Braccini, E.Galleani d'Agliano, F.Napoli, I.Pallecchi, A.S.Siri

INFM-LAMIA/CNR, Dipartimento di Fisica, Via Dodecaneso 33, 16146 Genova, Italy

P.Manfrinetti, A.Palenzona,

INFM, Dipartimento di Chimica e Chimica Industriale, Via Dodecaneso 31, 16146 Genova, Italy

(February 1, 2008)

Abstract

We present thermal conductivity measurements on very pure and dense bulk samples, as indicated by residual resistivity values as low as 0.5 mW cm and thermal conductivity values higher than 200 W/mK. In the normal state we found that the Wiedemann Franz law, in its generalized form, works well suggesting that phonons do not contribute to the heat transport. The thermal conductivity in the superconducting state has been analysed by using a two-gap model. Thank to the large gap anisotropy we were able to evaluate quantitatively intraband scattering relaxation times of π and σ bands, which depend on the disorder in different way; namely, as the disorder increases, it reduces more effectively the relaxation times of π than of σ bands, as suggested by a recent calculation [1].

1.INTRODUCTION

Since the discovery of MgB_2 [2], experimental findings established a phonon mediated s-wave superconductivity. Despite its standard origin, superconductivity in MgB_2 showed several unusual properties that can be ascribed to the presence of two gaps with different amplitudes emphasized by tunnelling and specific heat measurements. Theoretical studies [3] [4] pointed out that the peculiar electronic structure is the origin of this behaviour, being the larger gap, Δ_σ, associated with two-dimensional σ bands and the smaller one, Δ_π, associated with three-dimensional π bands. The two-gap model offers a simple explanation of several anomalies in the superconducting state [5] [6] [7]. Multiband effects due to the different parity of σ and π bands were predicted in the normal state, too [1], and, recently, have found confirmation in transport measurements [8]. Since interband impurity scattering turns out to be negligible, different bands behave as separate conduction channels in parallel and either σ or π channel prevails, depending on the disorder degree, being the clean (dirty) samples dominated by $\pi(\sigma)$ conduction.

In this paper we perform a quantitative analysis of thermal conductivity measurements

in the superconducting state to investigate the role of σ and π bands depending on the sample purity.

Thermal conductivity κ in the superconducting state among the other transport properties gives information on quasi-particle (QP) excitations and their dynamics with the advantage of probing only the QP response, since the superfluid does not carry heat. On the other hand, a major complication in the analysis of the thermal conductivity is often a substantial phonon contribution to the heat current. Consequently, the interpretation of experimental data can be ambiguous.

From a basic point of view, QP condensation below T_C causes a decreasing of the electron contribution to the thermal conductivity, κ_e, and an increasing of the phonon contribution, κ_p; thus κ below T_C can show a shoulder or a peak depending whether the heat current is dominated by electrons or phonons, and a more complex behaviour is exhibited when both the contribution are important.

From the beginning the thermal conductivity of MgB_2 showed the unexpected feature of not exhibiting any signature of the superconducting transition [9] [10] [11] [12]. This "anomaly" was initially ascribed to a perfect compensation of κ_e and κ_p [10] or to the presence of large thermal resistance at the grain boundaries [11]. As a matter of fact, the discovery that MgB_2 presents two gaps, one of which Δ_π is so small that QP condensation becomes exponential only below a reduced temperature of the order of $t = T/T_C \sim 0.2$, opened new perspectives in the interpretation of thermal conductivity data. Hence, the two gap model successfully used to fit specific heat data [5] can also be applied to the thermal conductivity to estimate the fraction of energy carried by the two bands, providing a useful mean to investigate multiband effects.

2.EXPERIMENTAL DETAILS

Dense (up to 2.4 g/cm^3, 90% of the theoretical density), clean and hard cylinder shaped samples have been prepared by a single step method [13] similar to the one reported in ref [14] [15]. Amorphous or crystalline B and Mg, put in Ta crucibles welded under argon and

closed in quartz tubes under vacuum, were heated up to 950°C . An X rays spectrum of a sample prepared by crystalline B is shown in fig. 1. All the peaks associated with the MgB_2 phase are present, no extra peaks due to the presence of free Mg , MgO, are detected. In the inset, SEM (Scanning Electron Microscopy) image of the same sample is shown. The image shows a network of well connected grains (2-4 mm large).

Two specimens were prepared for physical measurements: one from crystalline boron (MGB-1S) , one by using enriched ^{11}B (MGB11-1S). The samples were cut in the shape of parallelepiped bar (1×2-3×12 mm^3).

The thermal conductivity was measured using a steady state flux method with a heat flux sinusoidally modulated at low frequency (ν=0.003-0.01 Hz). Under these conditions the thermal conductivity is extracted as $\kappa = J(\nu)/\nabla T(\nu)$, where $J(\nu)$ is the heat flow provided at the frequency ν and $\nabla T(\nu)$ is the temperature gradient oscillating at the frequency ν. A small resistive heater (1×1 mm^2) is glued by GE varnish on the top end of the bar, being the bottom of the bar thermally connected with the sample holder. In such way a longitudinal heat flow is assured. The gradient applied to the sample was varied from 0.1 to 0.3 K/cm. Seebeck effect was measured simultaneously with the thermal conductivity providing a precise determination of the critical temperature.

3.RESULTS AND DISCUSSION

Resistivity measurements of the samples from 30 to 300 K are shown in fig. 2. In table 1 we report T_C^{onset}, the amplitude of the transition ΔT_C, $\rho(40K)$ and the residual resistivity ratio defined as $RRR = \rho(300K)/\rho(40K)$ for the two samples. The excellent quality of the samples is proved by the high T_C values (38.9, 38.7 K), the small ΔT_C values (0.2, 0.3 K), the low values of $\rho(40K)$ (0.6, 2.5 $\mu\Omega$cm) and the large values of RRR (7-15). Between the two samples the enriched ^{11}B (MGB11-1S) has the lower resistivity values which can mainly be ascribed to the very good quality of the Eagle-Picher enriched ^{11}B [15].

Thermal conductivity measurements of the two samples from 4 K to 250 K are shown in fig. 3. The outstanding quality and high density of the samples is evident from thermal

transport properties as well. Indeed, these samples have more than one order of magnitude higher thermal conductivities than polycrystalline samples [9] [10] [11]. In particular MGB11-1S exhibits a thermal conductivity as large as 215 W/Km at 65 K which is nearly two times higher than those of a single crystal [12], proving the excellent purity and density of this sample.

The thermal conductivity of MGB11-1S increases monotonically in the superconducting state, a change of slope is observable at about 8 K, while no signature of the superconducting transition is present; the normal state curve exhibits a pronounced maximum at about 70 K. Similar behaviour is presented by MGB-1S even if only data above 10 K are available.

The normal state behaviour of both samples is typical of a good metal in which the electron contribution to heat transport prevails. In order to estimate the relative weight of κ_e and κ_p we can consider the effective Lorenz number defined as $L_{eff} = \kappa\rho/T$. This quantity is assumed equal to $L_0 = 2.45 \times 10^{-8} W\Omega K^{-2}$ by the Wiedemann-Franz law (WFL); in good metals L_{eff} is equal to L_0 at low temperature where the electron impurity scattering prevails, then it decreases showing a minimum at about one tenth the Debye temperature Θ_D, deeper and deeper with increasing sample purity [16]; in dilute alloys where κ_p is not at all negligible L_{eff} becomes larger than L_0 and the ratio $L_{eff}/L_0 \simeq (1 + \kappa_p/\kappa_e)$ gives information on the relative weight of κ_e and κ_p [17]. In fig. 4 we plot L_{eff} for the two samples from 40 to 250 K. The curves exhibit the typical behaviour of good metals with slightly different levels of purity: at low temperatures the curves approach L_0 from below; they show a minimum at around 130 K ($\sim 0.1\Theta_D$, considering that in MgB_2 Θ_D $\sim$1000 K [18] [19]) which is more pronounced for MGB11-1S; finally, the curves increase towards L_0. Thus, we can conclude that in the normal state the WFL substantially works and κ_p can be neglected. Similar results were obtained also in sintered sample with low thermal conductivity [8], while different conclusions have been drawn on a single crystal [12], where a violation of the WFL was claimed. Actually, in a small sample with not well defined geometrical shape as a single crystal the geometrical factor which relates conductivity to conductance can be different in thermal and electrical measurement, giving an uncorrect

evaluation of the Lorenz number. In large bar cut specimens the geometrical factors can be estimated with better precision and more reliable verification of the WFL can be made.

In the superconducting state, since κ_p decreases as $(T/\Theta_D)^3$, we can assume that the thermal conductivity is dominated by electrons as well. Only at very low temperature $T \ll T_C$ due to QP condensation which decreases κ_e and enhances κ_p, their relative weight can change. Hence, we assume that lattice vibrations give negligible contribution to the thermal transport in the temperature region of our interest and in the following we analyse the thermal conductivity data in term of the electron contribution only.

The electron thermal conductivity in the superconducting state can be written as:

$$\kappa_e^s(T) = \kappa_e^n(T) g(t, \sigma) \tag{1}$$

where $\kappa_e^n(T)$ is the electron thermal conductivity in the normal state and $g(t, \sigma)$, for a given reduced gap, $\sigma = \Delta(0)/KT_C$, and reduced temperature, $t = T/T_C$, takes into account the QP condensation. The function $g(t, \sigma)$ was calculated in the framework of the BCS theory in the dirty and clean limit cases [20] [21] reproducing very well thermal conductivity in the low temperature superconductors. To analyse experimental data using eq. (1) two main problems have to be solved. First, eq. (1) has to be generalized to multiband conduction; second, $\kappa_e^n(T)$ has to be estimated. We start from the latter issue.

At low temperature, if the scattering with impurities prevails, $\kappa_e^n(T)$ can be obtained by the WFL, $\kappa_e^n(T) = L_0 T/\rho_0$ where ρ_0 is the residual resitivity. But in clean samples scattering with phonons has also to be considered. In ref. [8] this was done using a generalized WFL. We can write:

$$W_e = W_e^i + W_e^p \tag{2}$$

where, for the Matthiessen's rule, the thermal resistance $W_e = 1/\kappa_e$ is the sum of the thermal resistivity for scattering with impurities, W_e^i, and for scattering with phonons,W_e^p. Following ref. [16] we can write:

$$W_e^i = \frac{\rho_0}{L_0 T} \tag{3}$$

$$W_e^p = \frac{\rho_p(T)\left[\left(\frac{\Theta_D}{T}\right)^2 \frac{3}{\pi^2}\left(\frac{n_a}{2}\right)^{2/3}\right]}{L_0 T} \tag{4}$$

where $\rho_p(T) = 4\rho'\Theta_D\left(\frac{T}{\Theta_D}\right)^5 \int_0^{\Theta_D/T} \frac{x^5 dx}{(e^x-1)(1-e^{-x})}$ is given by the Bloch-Grüneisen equation, $\rho\prime$ is the temperature coefficient and n_a is the average number of electrons per unit cell in a given band.

Despite its simplicity, this model describes very well the normal state thermal conductivity of samples with very different degrees of disorder, with reasonable parameter values [8]; it contains the right features, vanishing to zero at low temperature linearly with T and requiring only three free parameters (ρ_0, Θ_D and $C = 4\rho'\Theta_D \frac{3}{\pi^2}\left(\frac{n_a}{2}\right)^{2/3}$) whose reliability can be checked by resistivity . The best fitting procedure is performed from 40 K to 200 K and the curves obtained with the parameter values listed in tab. 2 are reported in fig.4 as continuous lines. The theoretical curves fit the experimental data in the normal state in excellent way, while just below T_C, they lay above the data, decreasing linearly with temperature, where the experimental data start to decrease with larger slopes, due to the QP condensation. In tab. 2 we can see that the Θ_D and C values, which determine the intrinsic term , are nearly the same for both the samples, while the ρ_0 values change by a factor 4, as consequence of the different purity of the two samples; moreover we can see that the ρ_0 values are slightly lower than $\rho(40K)$ reported in table 1. Anyway, ρ_0, Θ_D and C values are in fair agreement with those obtained by fitting resistivity measurements [8].

Now we address the problem of generalizing eq. (1) in the case of multiband conduction. Following the approach used for the specific heat [5], we can write:

$$\frac{\kappa_e^s(T)}{\kappa_e^n(T)} = x g(t,\sigma_\pi) + (1-x) g(t,\sigma_\sigma) \tag{5}$$

where $\sigma_\pi = \Delta_\pi(0)/KT_C$ and $\sigma_\sigma = \Delta_\sigma(0)/KT_C$; the relative weights x and $(1-x)$ that in ref. [5] are related to the energy which condenses in each band, in our case rather represent the energy fractions carried by the π and σ bands, respectively; thus the relative weights take into account the mobility of the carriers in each band, also.

If we indicate with $\kappa_\pi^n(T) = x\kappa_e^n(T)$ and $\kappa_\sigma^n(T) = (1-x)\kappa_e^n(T)$ the thermal conductivity in the normal state of π and σ bands, eq. (5) states that the π and σ bands conduction occurs in parallel, as suggested by ref. [1].

Once a suitable g function is considered eq. (5) allows to fit the thermal conductivity data in the superconducting state with x, σ_π and σ_σ as free parameters. To describe σ and π QP we choose the g function in the dirty limit [20] in agreement with the fact that below 40 K $\kappa_e^n(T)$ is dominated by the scattering with impurities.

In figure 5 we show κ/T in the superconducting state for the two samples. The continuous line represents $\kappa_e^n(T)/T$, the dashed line represents $\kappa_e^s(T)/T$ given by eq. (5). The parameters obtained with the best fit procedure are summarized in table 2. We can see that the two-gap model provides an excellent agreement with the experimental data. We find σ_π=0.57 (0.6) and σ_σ=2.17 (1.9) for MGB11-1S (MGB-1S); these values, which correspond to $\Delta(0)_\pi = 1.9(2.0)\ meV$ and $\Delta(0)_\pi = 7.2(6.3)\ meV$ are in agreement with those found by specific heat data σ_π ∼0.6-0.65 and σ_σ ∼1.9-2.2. For the x parameter we find 0.85 and 0.75 for MGB11-1S and MGB-1S, respectively. From the specific heat analysis it comes out that the energy fraction which condenses in each band is roughly the same; thus our results imply that carriers in π bands are more mobile than in σ bands. The lacking signature of superconducting transition in thermal conductivity, naturally follows from the two-gap model; in fact, we find that the main contribution to heat transport comes from carriers in π bands whose strong condensation starts for $\sigma_\pi/t >> 1$ which means $t < 0.2$. In MGB11-1S data a change of slope occurs at about 8 K which in this framework represents the π QP condensation; in fact in figure 5 the dotted line represents $\kappa_e^s(T)/T$ given by eq. (5) with $x = 1$ and σ_π=0.57 . The curve fits well the data just below 10 K, while from 10 to 40 K also the σ QP excitations contribute to the transport.

The right weight of π and σ contributions to transport can be calculated for both samples by $\kappa_\pi^n(T) = x\kappa_e^n(T)$ and $\kappa_\sigma^n(T) = (1-x)\kappa_e^n(T)$ once the reliability of the x and $\kappa_e^n(T)$ evaluation has been verified. We point out that in the fit procedure, varying slightly the gap values, the quality of the fit does not change very much, while the x parameter for both the

samples is very well defined. On the other hand, below T_C, $\kappa_e^n(T) = L_0 T/\rho_0$ and therefore it only depends on the residual resistivity ρ_0 which can be experimentally estimated. So we can write:

$$\kappa_\pi^n(T) = L_0 T \frac{x}{\rho_0} = L_0 T \omega_{p_\pi}^2 \varepsilon_0 \tau_\pi^i \tag{6}$$

$$\kappa_\sigma^n(T) = L_0 T \frac{1-x}{\rho_0} = L_0 T \omega_{p_\sigma}^2 \varepsilon_0 \tau_\sigma^i \tag{7}$$

where ε_0 is the dielectric constant, $\omega_{p_{\pi,\sigma}}$ are the plasma frequencies and $\tau_{\pi,\sigma}^i$ are the intraband scattering relaxation times with impurities for π and σ bands.

Our fits state that carriers in π bands mainly contribute to carry heat. Indeed, the plasma frequency is larger for π than for σ bands [6] and this is enhanced in polycrystalline samples by averaging in the three direction. On the other hand, the scattering relaxation times change from sample to sample. Introducing in eq.s (6) and (7) the values of x and ρ_0 listed in tab. 2 and ω_{p_π}= 6.226 eV and ω_{p_σ}=3.403 eV [6] we obtain the scattering relaxation times for the two samples summarized in tab. 3. For MGB11-1S we find τ_π^i=2.2$\times 10^{-13}$ s and τ_σ^i=1.3$\times 10^{-13}$ s and the residual mean free paths $l_{\pi,\sigma}$=$\tau_{\pi,\sigma}^i v_{F\pi,\sigma}$, where $v_{F\pi,\sigma}$ are the averaged Fermi velocities for π an σ bands ($v_{F\pi}$=5.6$\times 10^5$ m/s and $v_{F\sigma}$=3.2$\times 10^5$ m/s [6]), come out l_π=1.2 $\times 10^{-7}$m and l_σ=4.1 $\times 10^{-8}$ m. These values are very large, exceeding the lattice constants by more than two orders of magnitude, indicating the excellent purity of this sample. For MGB-1S the relaxation rates are reduced, but the residual mean free paths are still large (l_π=2.9 $\times 10^{-8}$ m and l_σ=1.8 $\times 10^{-8}$ m).

Now we can look at the relaxation times in more details. In MGB11-1S $\tau_\pi^i > \tau_\sigma^i$, while in MGB-1S both the relaxation times are lower and $\tau_\pi^i < \tau_\sigma^i$. Practically, as the disorder increases, it reduces more effectively τ_π^i than τ_σ^i. Actually, it is not easy to say which kind of disorder is present in MGB-1S, being itself a quite pure sample. But typical defects in MgB_2 are vacancies or substitutions in the Mg site, which form more easily than in the B site. In these cases the relaxation rate for intraband impurity scattering is larger in π than in σ bands ($\tau_\pi^i < \tau_\sigma^i$) [1]. This prediction, which was well verified for large amount of defects [8], is here confirmed also going from very pure to rather pure samples.

This result can open new perspectives in thermal transport properties. In fact, as the disorder increases, we expect that the transport of σ bands prevails, and in superconducting state, the rapid QP condensation due to the large gap related to σ bands can become evident. Thus, in disordered samples, we expect that the thermal conductivity would diminish in absolute values, but it should show a wide shoulder below T_C. This fact, if true, is quite unusual, in fact the disorder generally smoothens, rather than enhancing features.

As a matter of fact, looking at the thermal conductivity data in literature, polycrystalline samples do not show more evident shoulder than clean samples. We think that polycrystalline samples, that surely are more disordered than single crystals or bulk samples, present resistive grain boundaries, which contribute to the thermal resistance masking the intrinsic behaviour of superconducting grains [11]. To emphasize the transport of carriers in σ bands by the progressive inhibition of transport in π bands, it is necessary to gradually introduce defects in pure samples. This can be done by suitable chemical substitution with the advantage of introducing a controlled amount of defects in a chosen site. Up to now, substituted samples have been obtained by sintering powders previously synthesized from the pure elements and such samples are not suitable for transport measurements. A second way is to introduce disorder by irradiation, but in this case the problem is to obtain a uniform defect distribution.

In conclusion, the role of disorder in MgB_2, which multiband effects make so peculiar, has been studied in pure samples by thermal transport measurements. We analysed in detail the thermal conductivity in the superconducting state, and thank to the large gap anisotropy we were able to evaluate quantitatively the intraband scattering relaxation times of π and σ bands.

Acknowledgement 1 *This work work is partially supported by the Istituto Nazionale per la Fisica della Materia through the PRA UMBRA*

REFERENCES

[1] I. I. Mazin, O. K. Andersen, O. Jepsen, O. V. Dolgov, J. Kortus, A. A. Golubov, A. B. Kuz'menko, D. van der Marel, cond-mat/0204013

[2] J.Nagamatsu, N.Nakagawa, T.Muranaka, Y.Zenitani and J.Akimitzu, Nature 410, 63 (2001).

[3] A.Y.Liu, I.I.Mazin and J.Kortus, Phys.Rev.Lett 87, 087005 (2001)

[4] H.J.Choi, D. Roundy, H. Sun, M. L. Cohen, S. G. Louie, cond-mat/0111182 and cond-mat/0111183

[5] F. Bouquet, Y. Wang, R. A. Fisher, D. G. Hinks, J. D. Jorgensen, A. Junod, N. E. Phillips, Europhysics Letters 56, 856 (2001).

[6] A. Brinkman, A.A. Golubov, H. Rogalla, O.V. Dolgov, J. Kortus, Y. Kong, O. Jepsen, O.K. Andersen Phys. Rev. B 65, 180517(R) (2002).

[7] A. A. Golubov, A. Brinkman, O. V. Dolgov, J. Kortus, O. Jepsen cond-mat/0205154

[8] M.Putti, V.Braccini, E.Galleani, F.Napoli, I.Pallecchi, A.S.Siri, P.Manfrinetti, A.Palenzona , Proceeding of BOROMAG, Genoa, 17-19 June (2002), Accepted for publication on Superc. Science Technol.

[9] T.Muranaka, J.Akimitsu, M.Sera, Phys.Rev. B 64, 020505R (2001).

[10] E.Bauer, Ch. Paul, St. Berger, S.Majumdar, H.Michor, M.Giovannini, A.Saccone, A.Bianconi, J. Phys.: Condens. Matter 13 (2001) L487-L493

[11] M.Putti, E.Galleani d'Agliano, D.Marrè, F.Napoli, M.Tassisto, P.Manfrinetti, A.Palenzona, Studies of High temperature Supeconductors, Ed. A.V.Narlikar, Vol. 38, 303 (2001)

[12] A.V. Sologubenko, J. Jun, S. M. Kazakov, J. Karpinski, H.R. Ott, Phys. Rev. B 66, 014504 (2002)

[13] A.Palenzona, P.Manfrinetti, V.Braccini, I.N.F.M. patent, N°TO2001A001098.

[14] D. K. Finnemore, J. E. Ostenson, S. L. Bud'ko, G. Lapertot, P. C. Canfield, Phys.Rev.Lett. 86, 2420 (2001).

[15] R. A. Ribeiro, S. L. Bud'ko, C. Petrovic, P. C. Canfield, cond-mat/0204510.

[16] R.Berman, Thermal conduction in solids, Clarendon Press, Oxford, (1976).

[17] M.Putti, Studies of High temperature Supeconductors, Vol.35 (2001) 281, Edited by A.Narlikar, Nova Science Publishers.

[18] C.Walti, E.Felder, C.Degen, G.Wigger, R.Monnier, B.Delley, H.R.Ott, Phys.Rev. B 64, 172515 (2001);

[19] F.Bouquet, R.A.Fisher, N.E.Phillips, D.G.Hinks, J.D.Jorgensen, Phys. Rev. Lett. 87, 047001 (2001).

[20] J.Bardeen, G.Rickayzen, L.Tewordt, Phys. Rev. 133 (1959) 982.

[21] B.T.Geilikman, M.I.Dushenat, V.R.Chechetkin, Sov. Phys. JEPT 46 (1977) 1213.

Figure captions

Figure 1. X-Rays pattern diffraction of an enriched ^{11}B bulk sample. The inset shows a SEM image of the same sample. The length scale of the picture is indicated in the bottom.

Figure 2. Resistivity measurements from 40 to 300 K.

Figure 3. Thermal conductivity measurements of the samples from 10 K to 250 K: the best fitting curves obtained with the parameter values listed in tab. 2 are reported as continuous lines.

Figure 4. The effective Lorenz number $L_{eff}/L_0 = \kappa\rho/(TL_0)$ from 40 to 250 K.

Figure 5. κ/T in the superconducting state. The continuous line represents the calculated κ_e^n/T; the dashed line represents κ_e^s/T given by eq. (5) with the parameter values summarized in tab. 2; the dotted line represents κ_e^s/T given by eq. (5) with $x = 1$ and σ_π

given in tab.2.

Table captions

Table 1. Critical temperature T_C^{onset}, amplitude of the transition ΔT_C, $\rho(40K)$ and residual resistivity ratio defined as $RRR = \rho(300K)/\rho(40K)$.

Table 2. Values of the parameters θ, ρ_0 and C obtained from the normal state thermal conductivity best fit and σ_π, σ_σ and x obtained by fitting eq. (5) with the superconducting state thermal conductivity.

Table 3. The intraband scattering time with impurities for π and σ bands, τ_π^i and $\tau_\sigma^i$and the residual mean free paths $l_{\pi,\sigma}$=$\tau_{\pi,\sigma}^i v_{F\pi,\sigma}$ ($v_{F\pi}$=5.6×10^5 m/s and $v_{F\sigma}$=3.2×10^5 m/s are the averaged Fermi velocities for π an σ bands [6]).

Table 1

sample	T_C^{onset}, K	$\Delta T_C, K$	$\rho(40K), \mu\Omega cm$	RRR
MGB11-1S	38.7	0.2	0.58	15.3
MGB-1S	38.9	0.3	2.1	7.1

Table 2

sample	θ, K	$\rho_0, \mu\Omega cm$	$C, \mu\Omega cm K^{-2}$	σ_π	σ_σ	x
MGB11-1S	1190	0.50	12	0.57	2.17	0.85
MGB-1S	1130	1.9	18	0.60	1.90	0.75

Table 3

sample	τ_π^i, s	τ_σ^i, s	l_π, m	l_σ, m
MGB11-1S	2.2×10^{-13}	1.3×10^{-13}	1.2×10^{-7}	4.1×10^{-8}
MGB-1S	0.5×10^{-13}	0.6×10^{-13}	2.9×10^{-8}	1.8×10^{-8}

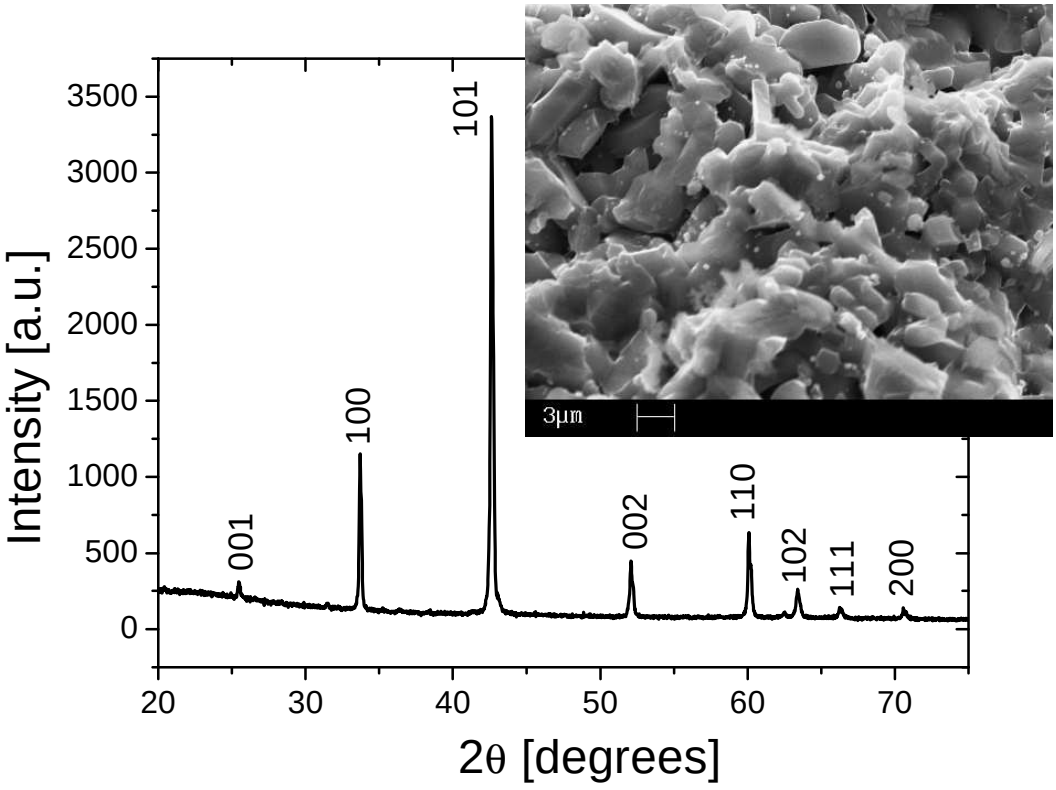
Intensity [a.u.]
2θ [degrees]
001
100
101
002
110
102
111
200
3µm

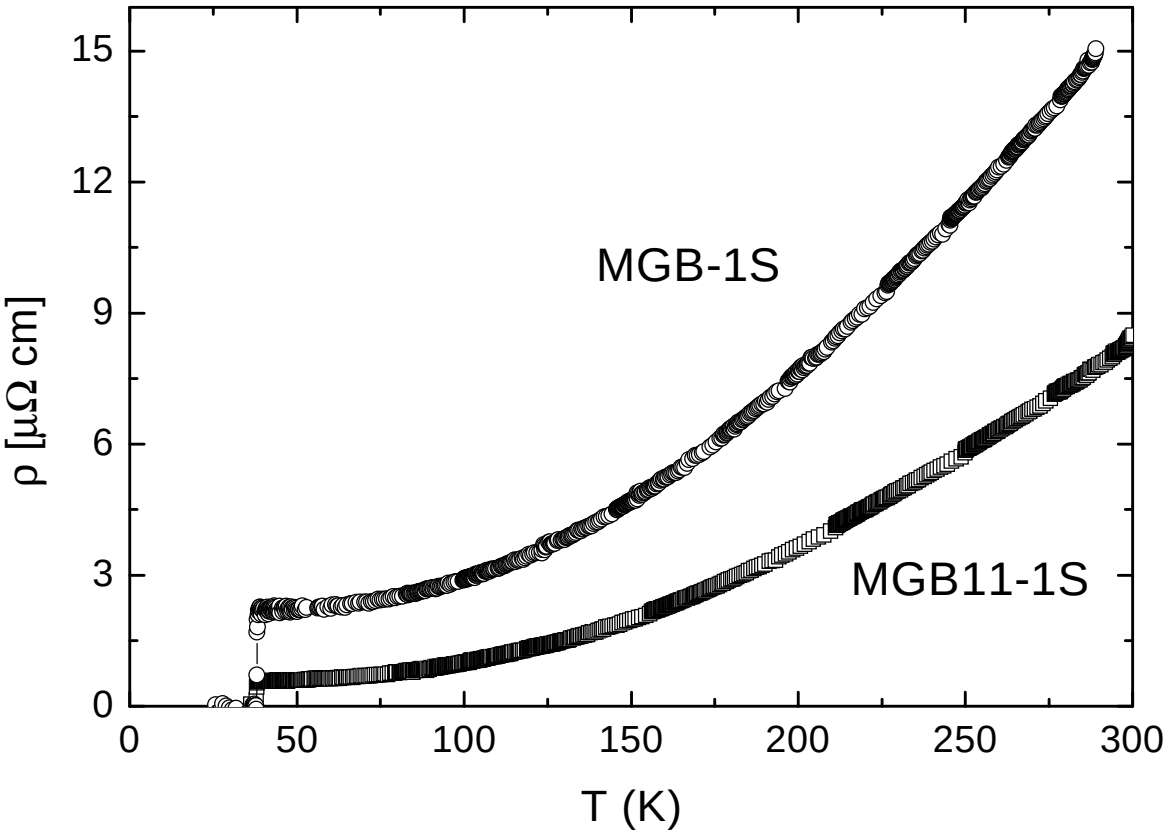
15
12
9
6
3
0
ρ [μΩ cm]
MGB-1S
MGB11-1S
0
50
100
150
200
250
300
T (K)

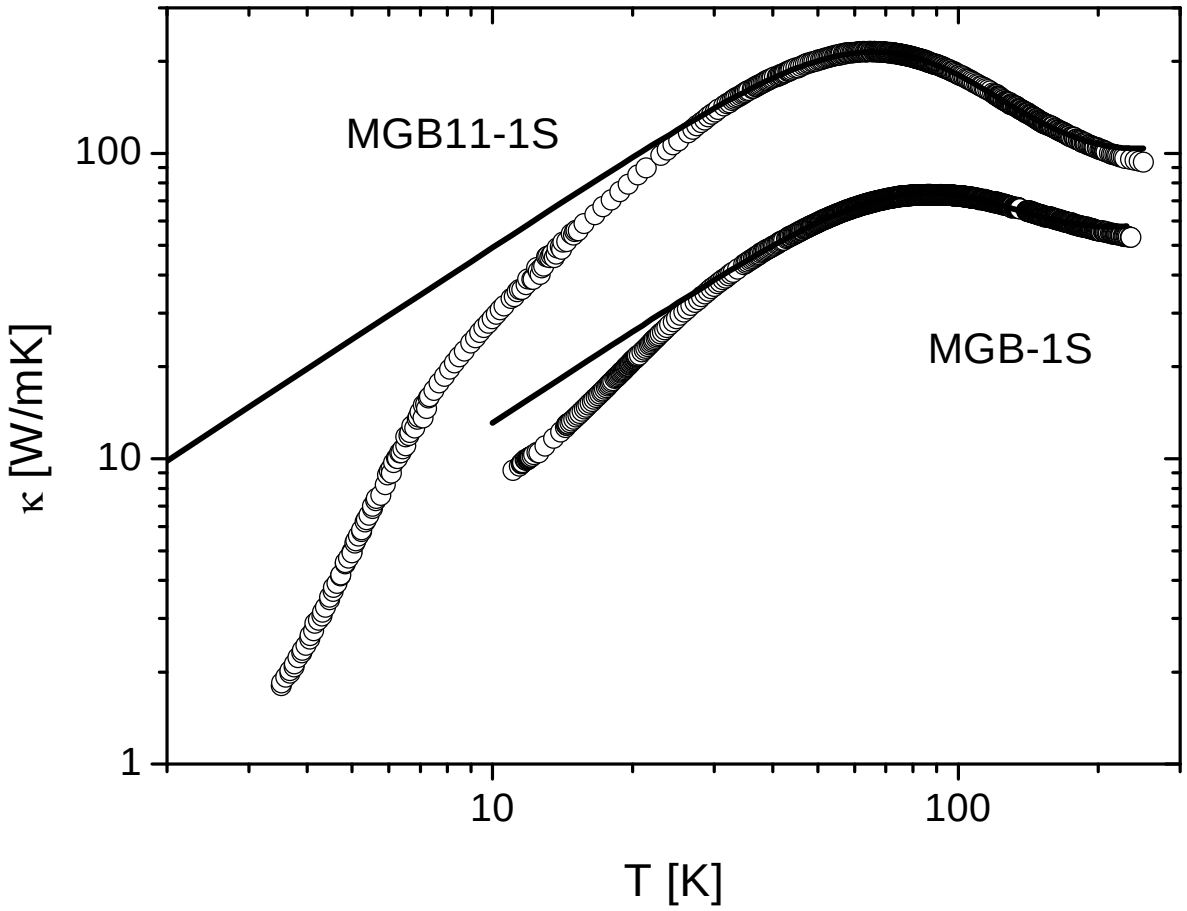
MGB11-1S
MGB-1S
100
10
1
κ [W/mK]
10
100
T [K]

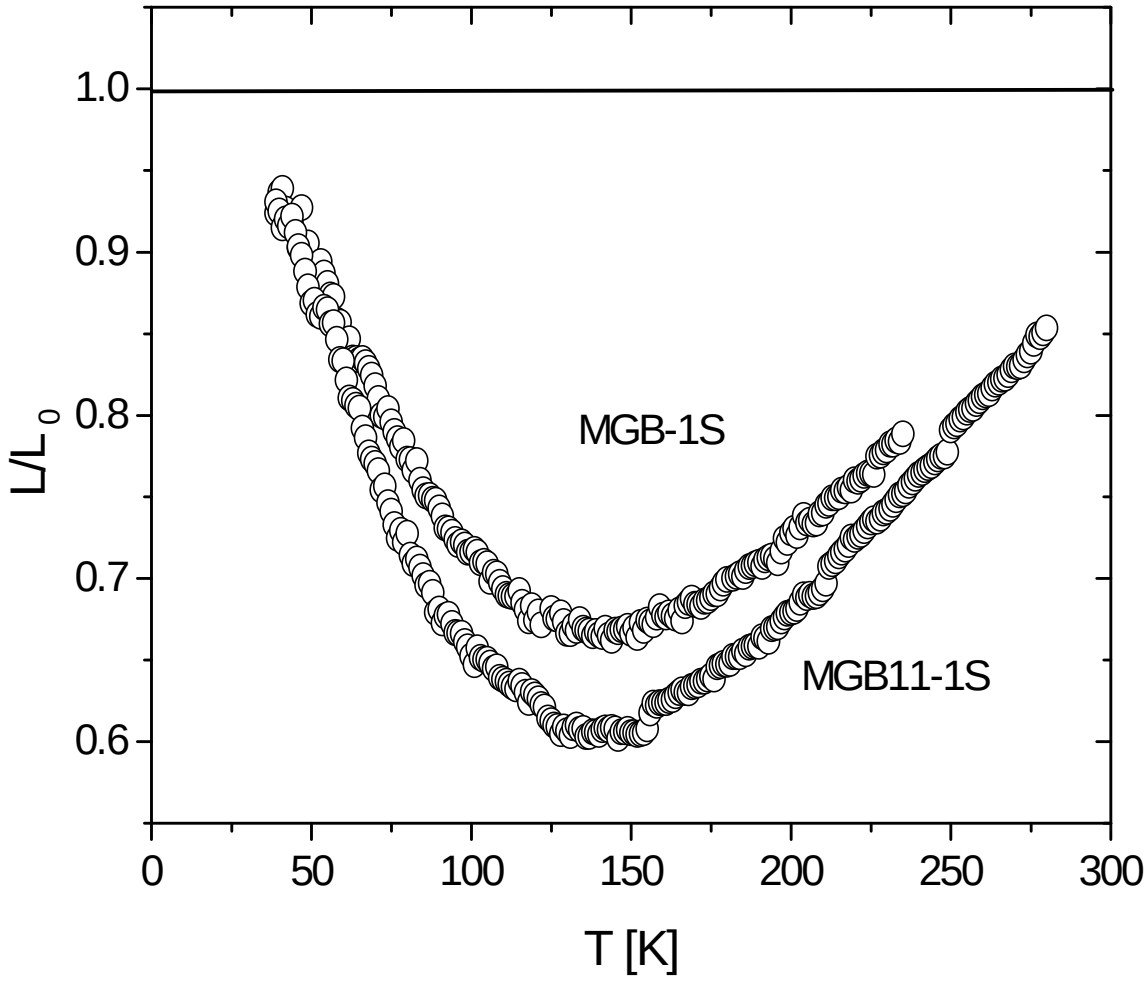
1.0
0.9
0.8
0.7
0.6
L/L0
MGB-1S
MGB11-1S
0
50
100
150
200
250
300
T [K]

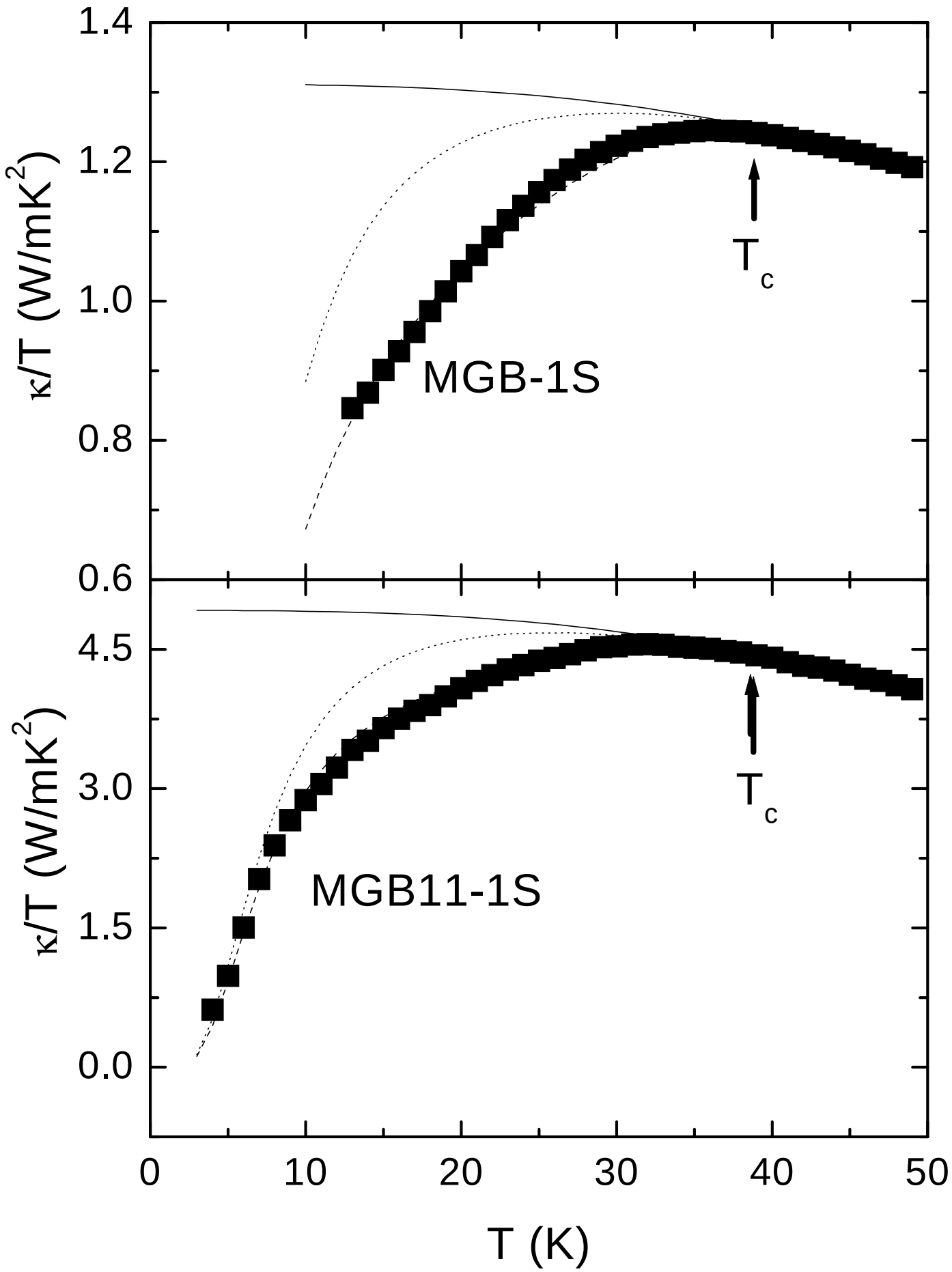
1.4
1.2
1.0
0.8
0.6
κ/T (W/mK²)
MGB-1S
T c
4.5
3.0
1.5
0.0
κ/T (W/mK²)
MGB11-1S
T c
0
10
20
30
40
50
T (K)